2015 IEEE/RSJ International Conference on Intelligent Robots and Systems (IROS)
Congress Center Hamburg
Sept 28 - Oct 2, 2015. Hamburg, Germany

# A Robust Nonlinear Controller for Nontrivial Quadrotor Maneuvers: Approach and Verification

Yuyi Liu, Jan Maximilian Montenbruck, Paolo Stegagno, Frank Allgöwer and Andreas Zell

*Abstract*— **This paper presents a nonlinear control approach for quadrotor Micro Aerial Vehicles (MAVs), which combines a backstepping-like regulator based on the solution of a certain class of global output regulation problems for the rigid body equations on SO(3), a robust controller for the system with bounded disturbances, as well as a trajectory generator using a model predictive control method. The proposed algorithm is endowed with strong convergence properties so that it allows the quadrotor MAVs to reach almost all the desired attitudes. The control approach is implemented on a high-payload-capable quadcopter with unstructured dynamics and unknown disturbances. The performance of our algorithm is demonstrated through a series of experimental evaluations and comparisons with another control method on normal and aggressive trajectory tracking tasks.**

## I. Introduction

Quadrotor Micro Aerial Vehicles (MAVs) are an area of keen interest because of their mechanical simplicity, vertical takeoff and landing (VTOL), potential to low-speed flight and capability of versatile tasks such as mapping [1], navigation [2], aerial acrobatics [3] and construction [4], among others.

From the control perspective, research has been carried out on the development of algorithms that can reach exceptional maneuverability [5] and improve the robustness of vehicles [6]. Previous work has also been done on trajectory planning [7] and formation of quadrotors [8]. The application of various control theories on quadrotors has been exploited, but major attention has been paid to constructing linear control systems such as proportional-derivative controllers [9] or linear backstepping controllers [10]. Nonlinear controllers, e.g. sliding mode [11] and Model Predictive Control (MPC) techniques [6], have been applied to MAVs, but most of them have been developed for linearized dynamics of a quadrotor. For instance, the learning-based MPC was flight tested in [12]. The MPC technique has been numerically validated on flying robots, while the expensive computation cost, despite of the successful tests on FPGAs [13], limits its implementation to on-board computers. Recent research on the development of a nonlinear controller on the special Euclidean group SE(3) [5], has provided MAVs with a novel geometric tracking method to track the motion in six Degrees-of-Freedom (DoFs) by continuously giving the desired position and attitude information for a quadrotor. This control algorithm is implemented and reported in [7], whose performance is impressive under accurate model identification. Other novel techniques, such as an output regulation approach for attitude control, have been proposed and proven for its strong convergence properties for almost all initial attitude conditions in [14], while this has not yet been tested in application.

In this paper, we focus on a robust nonlinear control algorithm based on the global output regulation technique for a nonlinear rigid-body system on Lie groups (extended from the approach in [14]). The proposed approach avoids the singularities that occur in other controllers not based on the representations of SO(3), and shows a strong convergence property in closed loop (we will show this in Section III-B). We further develop a regulation method based on the same technique for the goal of tracking the translational motion even under the influence of unstructured dynamics and unknown disturbances. The nonlinear control algorithm we introduce, with the help of an online trajectory planner based on an MPC method, provides a robust way even for the heavier and less agile MAVs to achieve nontrivial large attitude trajectories. In order to demonstrate the performance of the novel control algorithm, we also tested the state-of-the-art geometric tracking method (as introduced in [5] and tested in [7]) on our quadrotor platform on the exact same tracking tasks for the purpose of comparison.

The outline of this paper is as follows. In Section II, the dynamic model of a quadrotor MAV is first presented. Section III describes a nonlinear backstepping approach for the position and attitude control of a quadrotor with disturbance, including proofs revealing that our algorithms are asymptotically stable. An online trajectory planner using MPC for the waypoint or path tracking task is then introduced. Section IV explains in detail how the control approach is verified by an extensive experimental evaluation on trajectory tracking tasks and aggressive maneuvers, followed by the highlights of the actual experimental results and a comparison with an alternative control method. Finally, we present conclusions in Section V.

## II. Dynamic Model

We consider the quadrotor MAV as a rigid body model with six DoFs, which contains three DoFs describing translational motion and three describing the rotation of the quadrotor body frame with respect to the inertial frame. The

Y. Liu and A. Zell are with the Chair of Cognitive Systems, Department of Computer Science, University of Tübingen, Tübingen, Germany {yuyi.liu,andreas.zell}@uni-tuebingen.de

J. M. Montenbruck and F. Allgöwer are with the Institute for Systems Theory and Automatic Control, University of Stuttgart, Stuttgart, Germany {montenbruck,frank.allgower}@ist.uni-stuttgart.de

Y. Liu and P. Stegagno are with the Autonomous Robotics and Human-Machine Systems group, Max Planck Institute for Biological Cybernetics, Tübingen, Germany {yuyi.liu,paolo.stegagno}@tuebingen.mpg.de

978-1-4799-9994-1/15/$31.00 ©2015 IEEE

Equations of Motion are given by

$$\dot{x} = v, \tag{1a}$$
$$m\dot{v} = -mge_3 + RF + b, \tag{1b}$$
$$\dot{R} = RQ(\omega), \tag{1c}$$
$$J\dot{\omega} = -\omega \times J\omega + \tau, \tag{1d}$$

where $m$ is the mass of quadcopter, $x$ denotes the translational position, $g$ is the scalar value of the gravity acceleration, $e_3 = (0, 0, 1)^\top$. The nonconservative forces and moments in the body frame generated on the quadcopter by the aerodynamics of rotors are represented by $F$ and $\tau = (\tau_x, \tau_y, \tau_z)^\top$. The disturbance $b$ due to the external force and unstructured dynamics is considered in the form of an external force in the inertial frame. The inertial matrix $J$ in the body frame is computed via a simple CAD model of the quadrotor MAV used in the real experiment, with unknown mismatch to the actual values. $Q(\omega)$ is the skew-symmetric matrix form of the angular velocity $\omega = (\omega_1, \omega_2, \omega_3)^\top$ in the body frame cross product such that

$$Q(\omega) = \begin{bmatrix} 0 & -\omega_3 & \omega_2 \\ \omega_3 & 0 & -\omega_1 \\ -\omega_2 & \omega_1 & 0 \end{bmatrix}. \tag{2}$$

The rotation matrix $R$ represents the attitude of the quadrotor with respect to the inertial frame, which is an element of the special orthogonal group SO(3)$= \{R \in \mathbb{R}^{3\times3} | R^{-1} = R^\top, \ \det R = 1\}$.

We assume that the direction of the thrust $T$ on the quadcopter is along the $z$ axis of the body frame, the force vector $F$ has only its third entry non-zero that equals the total thrust of the four rotors, which is given by $F = (0, 0, T)^\top$ for non-negative $T \triangleq \sum_{i=1}^{4} f_i$, where the thrust of a single propeller is modeled as $f_i \triangleq c_T \omega_{t,i}^2$.

Taking the dynamic effects such as blade flapping not into consideration, we model the moments acting on the rigid body as

$$\begin{pmatrix} \tau_x \\ \tau_y \\ \tau_z \end{pmatrix} = \begin{pmatrix} d(f_4 - f_3) \\ d(f_2 - f_1) \\ \tau_{t,1} + \tau_{t,2} - \tau_{t,3} - \tau_{t,4} \end{pmatrix}, \tag{3}$$

where the reaction torque acting on the rigid body as $\tau_{t,i} \triangleq c_Q \omega_{t,i}^2$ are the fuctions of the speed $\omega_{t,i}$ of each rotor and the arm length $d$ of a quadrotor. The constant parameters $c_T$ and $c_Q$ are the thrust and drag coefficients determined by static thrust tests, respectively.

The final mapping from the rotor speeds into the forces and moments on a quadrotor can be described as

$$\begin{pmatrix} T \\ \tau_x \\ \tau_y \\ \tau_z \end{pmatrix} = \begin{bmatrix} c_T & c_T & c_T & c_T \\ 0 & 0 & -dc_T & dc_T \\ -dc_T & dc_T & 0 & 0 \\ c_Q & c_Q & -c_Q & -c_Q \end{bmatrix} \begin{bmatrix} \omega_{t,1}^2 \\ \omega_{t,2}^2 \\ \omega_{t,3}^2 \\ \omega_{t,4}^2 \end{bmatrix}. \tag{4}$$

The desired angular velocity of each motor, which is assumed as the control input on a quadrotor MAV by neglecting the error from the motor controller, therefore, can be obtained via solving the inverse of (4). The regulation approach to compute the desired nonconservative forces and moments on the quadrotor will be introduced in detail in Section III.

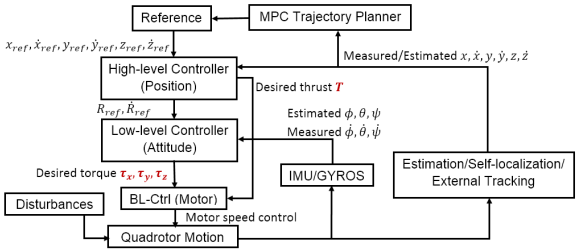


Fig. 1. The diagram of a complete control system for a quadrotor MAV.

## III. Control Approach

The complete proposed feedback control system for the quadrotor is illustrated in the block diagram in Figure 1.

On the promise of fulfilling various tasks, one can predescribe a set of references, which can either be a path or simply a waypoint far from the quadrotor. An on-board online trajectory planner (which we will introduce later) generates a trajectory so that later the quadrotor moves via tracking these references. The reference information, as well as the position and attitude data collected or estimated via reliable on-board hardware, algorithms or external motion capture systems, are passed to a control block, which outputs the desired rotation speed of each motor on the quadrotor via a cascaded position and attitude control algorithm and finally the transformation through Eq.(4). The details of the regulation algorithms for the quadrotor position and attitude are introduced in Section III-A and III-B respectively.

### A. Position Control

One position controller based on a nonlinear backstepping approach is first introduced here, which tracks the prescribed trajectory and outputs the desired thrust $F$ in the body frame plus the desired attitude, as well as the derivative of the desired attitude matrix for a lower level attitude tracker.

Subject to the first two equations in (1) but starting with an assumption of the full knowledge of external disturbances, we define the strongly convex cost function

$$P_1(x - x_{\text{ref}}) = \|(x - x_{\text{ref}})^\top K_0 (x - x_{\text{ref}})\|, \tag{5}$$

in order to specify the desired differential equation

$$\dot{x}_{\text{d}} - \dot{x}_{\text{ref}} = -\nabla P_1(x - x_{\text{ref}}), \tag{6}$$

where $x_{\text{d}}$ and $x_{\text{ref}}$ represents the desired quadrotor position resulting from the above gradient system and the exogenous reference position to track respectively, while $K_0 = \text{diag}(k_{0x}, k_{0y}, k_{0z})$ is a positive gain matrix (containing the diagonal elements denoting positive gains in each axis) for the position cost. The tracking error for the velocity and its derivative are accordingly given by

$$e_v = \dot{x} - \dot{x}_{\text{d}} = v - \dot{x}_{\text{ref}} + \nabla P_1(x - x_{\text{ref}}), \tag{7a}$$
$$\dot{e}_v = \dot{v} - \ddot{x}_{\text{ref}} + \nabla^2 P_1(x - x_{\text{ref}})(\dot{x} - \dot{x}_{\text{ref}}). \tag{7b}$$

Using a backstepping-like approach, we choose a Lyapunov function candidate

$$V_{\text{pos1}}(e_v, x) = \frac{1}{2} e_v^\top e_v + P_1(x - x_{\text{ref}}), \tag{8}$$

whose Lie derivative is rendered negative definite (under the assumption of full disturbance knowledge as we will see later) if $R$ equals $R_{\text{ref}}$ subject to

$$\begin{aligned} R_{\text{ref}} F \triangleq\ & mge_3 + b - m\nabla^2 P_1(x - x_{\text{ref}})(\dot{x} - \dot{x}_{\text{ref}}) \\ & + m\ddot{x}_{\text{ref}} - mKe_v - m\nabla P_1(x - x_{\text{ref}}) =: F', \end{aligned} \tag{9}$$

where $K = \operatorname{diag}(k_x, k_y, k_z)$ is a positive gain matrix (in the same structure as $K_0$) for the tracking error. A similar position control algorithm but under a no disturbance assumption ($b \triangleq 0$) has been introduced in [5].

However, such no disturbance assumption is not always practical for real implementations, especially under the condition that the reliable model identification or accurate estimate of external influence is not available. We, therefore, in the following do not impose the assumption of no disturbance for the purpose of robustness.

In our case, we regard the sum of the unstructured dynamics, internal disturbance and the external forces as the disturbance $b$ from the exogenous system, and we need an estimate of such disturbance, $b_{\text{est}}$, such that the disturbance error $e_b = \frac{1}{m}(b_{\text{est}} - b) \to 0$ for $t \to \infty$. Although still not in perfect practice, we further choose a Lyapunov function candidate

$$V_{\text{pos2}}(e_v, x) = V_{\text{pos1}}(e_v, x) + \frac{K_b^{-1}}{2} e_b^\top e_b, \tag{10}$$

under the assumption of a bounded external disturbance whose first derivative is negligible, which still works for a dynamic disturbance with trivial changes. $K_b$ denotes the gain diagonal matrix of the disturbance observer. The Lie derivative of $V_{\text{pos2}}(e_v, e_b, x)$ is rendered negative definite (as we will see later) subject to

$$\begin{aligned} \dot{b}_{\text{est}} &= mK_b(\dot{x} - \dot{x}_{\text{ref}}) + 2mK_bK_0(x - x_{\text{ref}}) \\ b_{\text{est}} &= \int_{-\infty}^{t} \dot{b}_{\text{est}}(\tau) d\tau, \end{aligned} \tag{11}$$

where $b_{\text{est}}$ can replace the external disturbance term $b$ in (9) in the closed-loop feedback system.

Considering that $R_{\text{ref}}$ in (9) is orthonormal and only the third entry of $F$, i.e. the thrust $T$, is nonzero, one must choose $T = \|F'\|$ in order to suffice (9). Therefore, the third column of $R_{\text{ref}} = \left[r^1_{\text{ref}}\ r^2_{\text{ref}}\ r^3_{\text{ref}}\right]$ can be solved from

$$r^3_{\text{ref}} = \frac{F'}{\|F'\|}, \tag{12}$$

and the other two columns of $R_{\text{ref}}$ can be filled orthonormally, for instance by a Gram-Schmidt process with candidates $r^3_{\text{ref}}$ from the previous equation and $r^1$, $r^2$ from the actual rotation $R = \left[r^1\ r^2\ r^3\right]$, i.e.

$$r^{2\prime}_{\text{ref}} = r^2 - \frac{r^2 \cdot r^3_{\text{ref}}}{r^3_{\text{ref}} \cdot r^3_{\text{ref}}} r^3_{\text{ref}}, \tag{13a}$$

$$r^2_{\text{ref}} = \frac{r^{2\prime}_{\text{ref}}}{\|r^{2\prime}_{\text{ref}}\|}, \tag{13b}$$

$$r^{1\prime}_{\text{ref}} = r^1 - \frac{r^1 \cdot r^3_{\text{ref}}}{r^3_{\text{ref}} \cdot r^3_{\text{ref}}} r^3_{\text{ref}} - \frac{r^1 \cdot r^2_{\text{ref}}}{r^2_{\text{ref}} \cdot r^2_{\text{ref}}} r^2_{\text{ref}}, \tag{13c}$$

$$r^1_{\text{ref}} = \frac{r^{1\prime}_{\text{ref}}}{\|r^{1\prime}_{\text{ref}}\|}, \tag{13d}$$

such that we obtain both the desired total thrust $T$ and the desired attitude $R_{\text{ref}}$ for the quadrotor control.

Here we prove the asymptotic stability of this position controller for $R = R_{\text{ref}} \triangleq \left[r^1_{\text{ref}}\ r^2_{\text{ref}}\ r^3_{\text{ref}}\right]$.

By sending $RF$ to $F'$, the closed-loop dynamics under the full disturbance knowledge assumption is given by

$$\begin{aligned} \dot{e}_v &= \dot{v} - \ddot{x}_{\text{ref}} + \nabla^2 P_1(x - x_{\text{ref}})(\dot{x} - \dot{x}_{\text{ref}}) \\ &= -ge_3 + \frac{1}{m} RF - \dot{v}_{\text{ref}} + \nabla^2 P_1(x - x_{\text{ref}})(\dot{x} - \dot{x}_{\text{ref}}) \\ &\triangleq -ge_3 - \dot{v}_{\text{ref}} + \nabla^2 P_1(x - x_{\text{ref}})(\dot{x} - \dot{x}_{\text{ref}}) + ge_3 + \dot{v}_{\text{ref}} \\ &\quad - \nabla^2 P_1(x - x_{\text{ref}})(\dot{x} - \dot{x}_{\text{ref}}) - Ke_v - \nabla P_1(x - x_{\text{ref}}) \\ &= -Ke_v - \nabla P_1(x - x_{\text{ref}}). \end{aligned} \tag{14}$$

The (directional) derivative of the chosen Lyapunov function candidate (8) is

$$\begin{aligned} \dot{V}_{\text{pos1}}(e_v, x) &= \nabla P_1(x - x_{\text{ref}}) \cdot (\dot{x} - \dot{x}_{\text{ref}}) + e_v \cdot \dot{e}_v \\ &= \nabla P_1(x - x_{\text{ref}}) \cdot (e_v - \nabla P_1(x - x_{\text{ref}})) \\ &\quad + e_v \cdot (-Ke_v - \nabla P_1(x - x_{\text{ref}})) \\ &= -\nabla P_1(x - x_{\text{ref}})^\top \nabla P_1(x - x_{\text{ref}}) - Ke_v^\top e_v < 0, \end{aligned} \tag{15}$$

hence (15) is negative definite.

In the next step, we consider the real environment without full knowledge of the disturbance generated from the unstructured dynamics and exogenous system. Still by sending $RF$ to $F'$, but replacing $b$ with $b_{\text{est}}$, the closed-loop dynamics is now given by

$$\begin{aligned} \dot{e}_v &= -\frac{1}{m}(b_{\text{est}} - b) - Ke_v - \nabla P_1(x - x_{\text{ref}}) \\ &= -Ke_v - \nabla P_1(x - x_{\text{ref}}) - e_b. \end{aligned} \tag{16}$$

The (directional) derivative of the Lyapunov function candidate (8) now turns

$$\begin{aligned} \dot{V}_{\text{pos1}}(e_v, x) &= -\nabla P_1(x - x_{\text{ref}})^\top \nabla P_1(x - x_{\text{ref}}) \\ &\quad - Ke_v^\top e_v - e_v^\top e_b, \end{aligned} \tag{17}$$

which is no longer negative definite for arbitrary disturbance error.

Considering the new Lyapunov function candidate (10) extended with a term of disturbance error, whose derivative, subject to a chosen derivative of disturbance as in (11), is

given by

$$\begin{aligned}\dot{V}_{\text{pos2}}(e_v, x) &= \dot{V}_{\text{pos1}}(e_v, x) + \frac{K_b^{-1}}{2} e_b^\top \dot{b}_{\text{est}} \\ &= -\nabla P_1(x - x_{\text{ref}})^\top \nabla P_1(x - x_{\text{ref}}) - K e_v^\top e_v \\ &\quad - e_v^\top e_b + \frac{K_b^{-1}}{2} e_b^\top \dot{b}_{\text{est}} \\ &= -\nabla P_1(x - x_{\text{ref}})^\top \nabla P_1(x - x_{\text{ref}}) - K e_v^\top e_v < 0,\end{aligned} \tag{18}$$

Therefore, (18) is negative definite, which proves the asymptotical stability of the proposed position control algorithm.

### *B. Attitude Control*

In this section, we introduce a control method for the tracking of the attitude $R$ of the quadrotor with strong convergence properties. The specific approach is based on the solution of a class of output regulation problems which contains the rotational motion for a rigid body. The tracking error is given by $E = RR_{\text{ref}}^\top$, where $R$ corresponds to the rotation matrix describing the current attitude, and $R_{\text{ref}}$, computed via the approach introduced in Section III-A, represents the desired attitude. We also assume the error between the current and a desired angular velocity in body frame as

$$e_\omega = Q(\omega) - Q(\omega_{\text{d}}). \tag{19}$$

The goal of the attitude controller is to regulate the output of the quadrotor attitude $(E, e_\omega) \to (I, 0)$ for $t \to \infty$, which implies $R \to R_{\text{ref}}$ and $Q(\omega) \to Q(\omega_{\text{d}})$ for $t \to \infty$.

We employ a backstepping method analogous to the position controller for the attitude regulation. Based on the proof in [15], a cost function $P_2(E) = \frac{1}{2}\operatorname{tr}((E-I)^\top(E-I)) = n - \operatorname{tr}(E)$, which has

$$\operatorname{grad} P_2(E) = \frac{1}{2}(E - E^\top)E, \tag{20}$$

can be chosen, where $\operatorname{grad} P_2$ is the projection of $\nabla P_2$ onto tangent spaces of SO(3). Here we assume a cost function for the quadrotor rotation in form of

$$P_2(E) = 3 - \operatorname{tr}(E). \tag{21}$$

The derivative of the rotational error $E$ becomes

$$\dot{E} = \dot{R}R_{\text{ref}}^\top + R\dot{R}_{\text{ref}}^\top \triangleq -k_{\text{rot}} \operatorname{grad} P_2(E), \tag{22}$$

where $k_{\text{rot}}$ is a positive gain for the cost of rigid body rotation.

By employing Eq. (1c), the desired angular velocity of the quadrotor is given by

$$Q(\omega_{\text{d}}) = -\frac{k_{\text{rot}}}{2}(R_{\text{ref}}^\top R - R^\top R_{\text{ref}}) - \dot{R}_{\text{ref}}^\top R_{\text{ref}}, \tag{23}$$

which is obtained from (22):

$$\begin{aligned}&RQ(\omega_{\text{d}})R_{\text{ref}}^\top \triangleq -k_{\text{rot}} \operatorname{grad} P_2(E) - R\dot{R}_{\text{ref}}^\top \\ &Q(\omega_{\text{d}}) \triangleq R^\top(-k_{\text{rot}} \operatorname{grad} P_2(E))R_{\text{ref}} - R^\top R\dot{R}_{\text{ref}}^\top R_{\text{ref}} \\ &= -k_{\text{rot}} R^\top \frac{1}{2}(RR_{\text{ref}}^\top - R_{\text{ref}}R^\top)RR_{\text{ref}}^\top R_{\text{ref}} - \dot{R}_{\text{ref}}^\top R_{\text{ref}}.\end{aligned} \tag{24}$$

The derivative of the desired angular velocity computed from (23) is

$$\begin{aligned}Q(\dot{\omega}_{\text{d}}) &= \frac{d}{dt}\left\{-\frac{k_{\text{rot}}}{2}(R_{\text{ref}}^\top R - R^\top R_{\text{ref}}) - \dot{R}_{\text{ref}}^\top R_{\text{ref}}\right\} \\ &= -\frac{k_{\text{rot}}}{2}(\dot{R}_{\text{ref}}^\top R + R_{\text{ref}}^\top \dot{R} - \dot{R}^\top R_{\text{ref}} - R^\top \dot{R}_{\text{ref}}) \\ &\quad - \ddot{R}_{\text{ref}}^\top R_{\text{ref}} - \dot{R}_{\text{ref}}^\top \dot{R}_{\text{ref}}.\end{aligned} \tag{25}$$

Considering Eqs. (1d) and (25), we obtain the derivative of the angular velocity error represented by

$$\begin{aligned}\dot{e}_\omega &= Q(\dot{\omega}) - Q(\dot{\omega}_{\text{d}}) \\ &= Q(J^{-1}(-\omega \times J\omega + \tau)) + \ddot{R}_{\text{ref}}^\top R_{\text{ref}} + \dot{R}_{\text{ref}}^\top \dot{R}_{\text{ref}} \\ &\quad + \frac{k_{\text{rot}}}{2}(\dot{R}_{\text{ref}}^\top R + R_{\text{ref}}^\top \dot{R} - \dot{R}^\top R_{\text{ref}} - R^\top \dot{R}_{\text{ref}}).\end{aligned} \tag{26}$$

For a backstepping approach for the rigid body rotation, we choose a Lyapunov function candidate

$$V_{\text{att}}(E, e_\omega) = \frac{1}{2}Q^{-1}(e_\omega)^\top Q^{-1}(e_\omega) + P_2(E), \tag{27}$$

whose Lie derivative, similar as the position controller we introduced in Sec. III-A, is rendered negative definite (as we will prove later) if $\tau$ equals $\tau_{\text{d}}$ subject to

$$\begin{aligned}\tau_{\text{d}} = JQ^{-1}\Big(&-k_\omega e_\omega - \frac{k_{\text{rot}}}{2}\Big[\dot{R}_{\text{ref}}^\top R + R_{\text{ref}}^\top \dot{R} - \dot{R}^\top R_{\text{ref}} \\ &- R^\top \dot{R}_{\text{ref}}\Big] - \ddot{R}_{\text{ref}}^\top R_{\text{ref}} - \dot{R}_{\text{ref}}^\top \dot{R}_{\text{ref}} - 2R_{\text{ref}}^\top R\Big) + \omega \times J\omega,\end{aligned} \tag{28}$$

where $k_\omega$ is a positive gain for the tracking error of the quadrotor angular velocity. The derivative $\dot{R}$ can be obtained by introducing the current attitude $R$ into Eq. (1c), while $R_{\text{ref}}$ inherits from the results of Eqs. (12) and (13). Under the assumption that $\ddot{R}_{\text{ref}}$ equals 0, we only compute the derivative of quadrotor desired attitude $\dot{R}_{\text{ref}}$ from Eq. (9) through the following process:

In case the jerk of the desired trajectory is assumed always zero, the (closed) derivative of $F'$ in (9) is

$$\begin{aligned}\dot{R}_{\text{ref}}F &\triangleq \frac{d}{dt}\left(mge_3 - m\nabla^2 P_1(x - x_{\text{ref}})(\dot{x} - \dot{x}_{\text{ref}})\right. \\ &\quad \left. + m\ddot{x}_{\text{ref}} - mke\right) \\ &= -m(2k_0 + k)(\ddot{x} - \ddot{x}_{\text{ref}}) - 2mk_0 k(\dot{x} - \dot{x}_{\text{ref}}) =: \dot{F}',\end{aligned} \tag{29}$$

from which the reference angular velocity is computed using (1c),

$$Q(\omega_{\text{ref}})F = R_{\text{ref}}^\top \dot{F}'. \tag{30}$$

Recalling the third column entry of $Q(\omega)$ in (2), one can obtain the reference roll and pitch rate in form of

$$\omega_{1,\text{ref}} = -\frac{(R_{\text{ref}}^\top \dot{F}')^2}{\|F'\|}, \tag{31a}$$

$$\omega_{2,\text{ref}} = \frac{(R_{\text{ref}}^\top \dot{F}')^1}{\|F'\|}. \tag{31b}$$

Considering that in most cases the yaw attitude is required as the camera front direction (or zero for the quadrotor with

no vision-based equipment) and no specific desired yaw rate is required for the quadrotor flight, one can constantly define the value of $\omega_{3,\text{ref}} = \frac{1}{2}(\psi_{\text{ref}} - \psi_{\text{current}})$ for the reference and current yaw attitude $\psi$ at every moment, and $\dot{R}_{\text{ref}}$, therefore, can be solved via Eq. (1c).

Analogous to the derivations for the position controller, we prove here the asymptotic stability of the backstepping regulation method for attitude control for $\tau = \tau_{\text{d}}$.

By sending $\tau$ to Eq. (1d), the closed loop dynamics for rigid body rotation is given by

$$\begin{aligned}\dot{e}_\omega \triangleq\ & Q\Big(J^{-1}\Big(-\omega\times J\omega + \omega\times J\omega + JQ^{-1}\Big(-2R_{\text{ref}}^\top R \\ & - k_\omega e_\omega - \frac{k_{\text{rot}}}{2}\Big[\dot{R}_{\text{ref}}^\top R + R_{\text{ref}}^\top\dot{R} - \dot{R}^\top R_{\text{ref}} - R^\top\dot{R}_{\text{ref}}\Big] \\ & - \ \ddot{R}_{\text{ref}}^\top R_{\text{ref}} - \dot{R}_{\text{ref}}^\top\dot{R}_{\text{ref}}\Big)\Big) + \ddot{R}_{\text{ref}}^\top R_{\text{ref}} + \dot{R}_{\text{ref}}^\top\dot{R}_{\text{ref}} \\ & + \frac{k_{\text{rot}}}{2}\Big[\dot{R}_{\text{ref}}^\top R + R_{\text{ref}}^\top\dot{R} - \dot{R}^\top R_{\text{ref}} - R^\top\dot{R}_{\text{ref}}\Big] \\ =\ & -k_\omega e_\omega - 2R_{\text{ref}}^\top R.\end{aligned} \tag{32}$$

The (directional) derivative of the chosen Lyapunov function candidate (27), is

$$\begin{aligned}&\dot{V}_{\text{att}}(E,e_\omega) = Q^{-1}(e_\omega)^\top Q^{-1}(\dot{e}_\omega) + \operatorname{grad} P_2(E)\cdot\dot{E} \\ &= Q^{-1}(e_\omega)^\top Q^{-1}(-k_\omega e_\omega - 2R_{\text{ref}}^\top R) + \operatorname{grad} P_2(E)\cdot\dot{E} \\ &= -Q^{-1}(e_\omega)^\top Q^{-1}(2R_{\text{ref}}^\top R) - k_\omega Q^{-1}(e_\omega)^\top Q^{-1}(e_\omega) \\ &\quad + \operatorname{grad} P_2(E)\cdot\dot{E}.\end{aligned} \tag{33}$$

Considering the property $x^\top y = -\frac{1}{2}\operatorname{tr}[Q(x)Q(y)]$ for any two vectors, we can reach

$$Q^{-1}(e_\omega)^\top Q^{-1}(2R_{\text{ref}}^\top R) = -\frac{1}{2}\operatorname{tr}(e_\omega 2R_{\text{ref}}^\top R), \tag{34}$$

by applying Eqs. (22) and (34), Eq. (33) is given by

$$\begin{aligned}&\dot{V}_{\text{att}}(E,e_\omega) = -k_\omega Q^{-1}(e_\omega)^\top Q^{-1}(e_\omega) - \operatorname{tr}(\dot{E}) \\ &\quad + \frac{1}{2}\operatorname{tr}(e_\omega 2R_{\text{ref}}^\top R) \\ &= -k_\omega Q^{-1}(e_\omega)^\top Q^{-1}(e_\omega) + \frac{1}{2}\operatorname{tr}(e_\omega 2R_{\text{ref}}^\top R - 2\dot{E}) \\ &=: \dot{V}_{\text{att},1} + \dot{V}_{\text{att},2},\end{aligned} \tag{35}$$

where $\dot{V}_{\text{att},1} = -k_\omega Q^{-1}(e_\omega)^\top Q^{-1}(e_\omega) \leqslant 0$.

We therefore only focus on the rest term $\dot{V}_{\text{att},2}$ in (35) since $\dot{V}_{\text{att},1}$ is negative semi-definite (proved in [14]),

$$\begin{aligned}\dot{V}_{\text{att},2} &= \frac{1}{2}\operatorname{tr}(e_\omega 2R_{\text{ref}}^\top R - 2\dot{E}) \\ &= \frac{1}{2}\operatorname{tr}\Bigg(\Bigg(R^\top\dot{R} + \frac{k_{\text{rot}}}{2}(R_{\text{ref}}^\top R - R^\top R_{\text{ref}}) \\ &\quad + \dot{R}_{\text{ref}}^\top R_{\text{ref}}\Bigg)2R_{\text{ref}}^\top R - 2\dot{R}R_{\text{ref}}^\top - 2R\dot{R}_{\text{ref}}^\top\Bigg) \\ &= \frac{1}{2}\operatorname{tr}(k_{\text{rot}}(R_{\text{ref}}^\top R R_{\text{ref}}^\top R - I)) \\ &= \frac{k_{\text{rot}}}{2}\operatorname{tr}((E^\top - E)E^\top) = \frac{k_{\text{rot}}}{2}\operatorname{tr}(E(E - E^\top)) \\ &= \frac{k_{\text{rot}}}{4}\operatorname{tr}((E - E^\top)^2) < 0,\end{aligned} \tag{36}$$

hence (33) is negative definite.

### C. Trajectory Planning

A trajectory planning algorithm based on an MPC method is used to generate a prescribed trajectory for the quadrotor vehicles. This planner sets the jerks in three dimensions as the inputs for three optimal control problems (OCPs) split from a coupled problem originally describing the quadcopter motion. The state in each problem consists of the position, velocity and acceleration along three axes respectively. Considering with a sampling time $\Delta t$, for each decoupled axis, the discrete time states $z$ and inputs $u$ at $k^{\text{th}}$ step are given by

$$u[k] = \dddot{x}(k\Delta t) \tag{37a}$$

$$z[k] = [x(k\Delta t)\ \dot{x}(k\Delta t)\ \ddot{x}(k\Delta t)]^\top \tag{37b}$$

$$z[k+1] = Az[k] + Bu[k] \tag{37c}$$

$$A = \begin{bmatrix}1 & \Delta t & \frac{1}{2}\Delta t^2 \\ 0 & 1 & \Delta t \\ 0 & 0 & 1\end{bmatrix} \tag{37d}$$

$$B = [\frac{1}{6}\Delta t^3\ \frac{1}{2}\Delta t^2\ \Delta t]^\top. \tag{37e}$$

Each OCP can be described with a quadratic cost function

$$\begin{aligned}\min J = &\sum_{k=0}^{N}(u[k]^\top P u[k] + d_z[k]^\top L_{\text{s}} d_z[k]) \\ &+ d_z[N+1]^\top L_{\text{t}} d_z[N+1],\end{aligned} \tag{38}$$

subject to the dynamics explained above and corresponding boundary conditions

$$j_{\min} \leq \dddot{x}[k] \leq j_{\max}, \tag{39a}$$

$$a_{\min} \leq \ddot{x}[k] \leq a_{\max}, \tag{39b}$$

where $N$ represents the receding horizon, $d_z[k]$ denotes the error between state and given reference, and $P$, $L_{\text{s}}$ and $L_{\text{t}}$ are the weights of input cost, stage state cost and terminal state cost, respectively. The described small convex OCPs are solved via CVXGen [16] using the interior point method. In [17] the authors introduced a similar linearization technique to build the quadrotor model, while they predicted a diminishing horizon trajectory with terminal constraints for the state interception purpose.

By using adaptive cost weight settings, the planner generates a locally optimal trajectory from a given path or simply a waypoint. For a waypoint tracking task, the weight of terminal state cost is automatically set dominant, while the weight of all stage state costs is set to zero. In contrast, for a path tracking task, the weight of terminal cost is set to zero. Differently from the normal MPC approach where the first step control input $u[0]$ is used as the input for the system, only the first predicted time-relevant states (as $z[1]$ in three OCPs) are passed into the controller introduced in Sec. III-A. In case that no feasible locally optimal solution is available, the planner automatically loads the last previous feasible solution to avoid an "unstable" trajectory.

## IV. VERIFICATION

The control algorithm presented herein has been validated numerically in MATLAB, ROS/Gazebo physical simulations of a multi-rotor model with parametric mismatch and uncertain disturbances, and finally through real tests. Our results are compared with the results obtained using the geometric tracking algorithm [5]. We do not report the results of the simulations for the sake of brevity.

### A. Experiment Configuration

A series of experiments have been carried out on a modified Quadro-XL quadrotor MAV from MikroKopter. The quadrotor is equipped with an Odroid-XU board with Cortex™ $A15$ quad-core CPUs. The Quadro-XL is chosen because of its ability to carry a payload up to $1.0$ kg except battery. Hence, it is suitable to carry an on-board computer and stereo cameras for versatile tasks that require high autonomy and vision techniques such as mapping and target tracking in an unknown GPS-denied environment.

Within the tests, the control algorithm has been implemented within the ROS-based TeleKyb framework [18]. The quadrotor position has been recorded via an external motion capture system and been passed into the on-board computer at a sampling frequency of $120$ Hz over a wireless channel, while the other essential data i.e. linear acceleration, orientation and angular velocity of the quadrotor, have been collected by a low-cost on-board Inertial Measurement Unit (IMU). The on-board computer performs the computation of control algorithms with the use of the collected and filtered data, and generates the regulated motor commands at $100$ Hz, while the MPC-based trajectory planner, due to an average computational cost of $9$ ms, is executed at $50$ Hz with a horizon of $1$ s. The overall vehicle, equipped with a $5000$ mAh LiPo battery, an on-board computer, WiFi communications and all sensors except stereo cameras, weighs $1.588$ kg. However, we set the nominal mass to $1.5$ kg during the experiments. These parametric mismatches plus the unknown hardware and external disturbance are added to check the robustness property of our method.

In order to validate our proposed trajectory tracking algorithm and to demonstrate its capability of nontrivial trajectory maneuvers experimentally, we evaluated the quadrotor with a similar reference eight-shape path as in [19], which was parameterized as

$$P_d(t) = R_x(\frac{\pi}{6})R_z(\frac{\pi}{12}) \begin{bmatrix} \frac{\sin(\sigma(t))\cos(\sigma(t))}{\sin(\sigma(t))^2+1} \\ \frac{\cos(\sigma(t))}{\sin(\sigma(t))^2+1} \\ 0 \end{bmatrix} + \begin{bmatrix} 0 \\ 0 \\ 1.2 \end{bmatrix}, \tag{40}$$

where $R_x$ and $R_z$ denote the rotation matrices along $x$ and $z$ axis respectively, while $\sigma(t)$ is a function whose derivative is given by

$$\dot{\sigma}(t) = V\sqrt{\sin^2 t + 1}. \tag{41}$$

The prescribed trajectory provided the quadrotor with a eight-shape flight at a constant speed of $V$ m/s, as the dotted black line shown in Fig. 2.

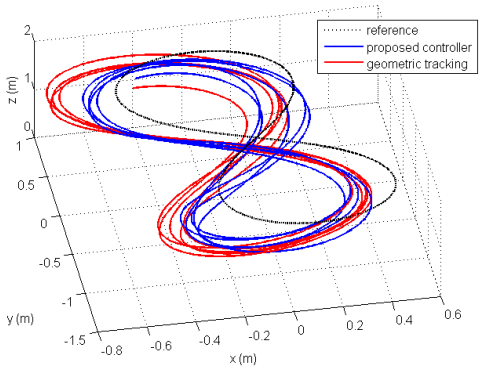


Fig. 2. Resulting flight of an eight-shape trajectory for proposed controller and geometric tracking controller. The dotted black line represents the reference path. The solid blue line represents the actual quadrotor trajectory using the proposed control method. The solid red line represents the compared flight using the geometric tracking method.

By deriving the position reference in (40), we obtained the analytic solutions of the velocity and acceleration references. When the quadrotor flew with a geometric tracking controller, we imported these references for the controller to track. When testing our proposed algorithm, we only passed the position reference (40) into the onboard computer and utilized the online planner to automatically generate full required state references for each feedback step.

### B. Experiment Results

We first tested the robustness of our proposed controller and compared it with the results using geometric tracking algorithm via an easy task that required the quadrotor to fly from a start point $(0.5, 0.5, 1.3)$ to $(0, 0, 1)$ and kept hovering for $25$ s. The steady state of the quadrotor is with a pitch angle at $3^\circ$ due to the parametric mismatches and disturbances. The translational error on each axis are illustrated in Fig. 3. The norm of the resulting Mean Square Errors (MSE) on position for our proposed method is $1.51$ cm, while the MSE with the geometric tracking algorithm reaches $4.14$ cm. There exist translational offsets on three axes up to $20$ cm for the geometric tracking algorithm. We chose relatively conservative control gain settings on both controllers for the purpose of more stable large-angle maneuvers. With the geometric tracking controller, a more aggressive gain setting can reduce the translational offsets but lead to a risk of instability when achieving the nontrivial trajectory tracking task.

In the second experiment, the quadrotor was first commanded to initially take off and hover at a start point at $1.5$ m height. The reference trajectory was then imported into the controller to achieve the repeated eight-shape flight task for $24$ s at $1.2$ m/s. We performed this test with both control methods (Fig. 4).

Fig. 2 shows a comparison of the quadrotor position during this tracking task between the geometric tracking method and the proposed method. The blue line represents the resulting trajectory with our proposed method, which can be observed closer to the red reference trajectory when compared to the trajectory with geometric tracking method

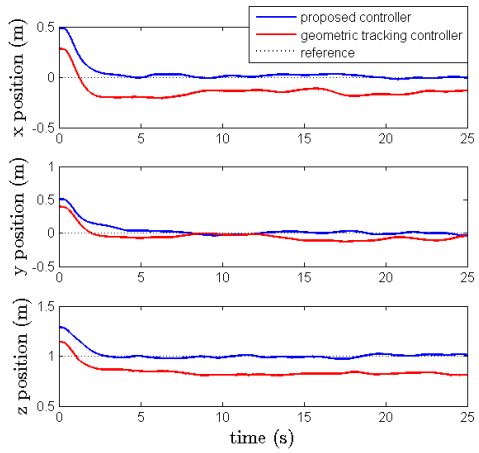


Fig. 3. Resulting quadrotor response for a hovering task. The reference position is set to (0,0,1). The dotted black line represents the reference command. The solid blue line represents the quadrotor position with our proposed control method. The solid red line is the quadrotor position with the geometric tracking controller.

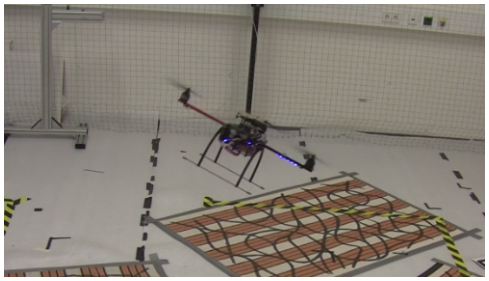

Fig. 4. "Nontrivial maneuvers" experiment. The quadrotor, using the proposed controller in this paper, is tracking an eight-shape trajectory with a maximum tilt up to $40°$.

(the green line). The maximum tilt of the quadrotor within this large-angle trajectory reached over $40°$. In addition, we can have an intuitive comparison on the performance of two controllers from the translational errors, as shown in Fig. 5. For this aggressive maneuver task, the translational MSE for our proposed method is 3.37 cm, while the MSE with the geometric tracking algorithm reaches 6.14 cm.

## V. Conclusions

In this paper, we have proposed a new nonlinear control strategy for multi-rotor MAVs that allows for online trajectory decision and nontrivial maneuvers tracking with robustness. We have also shown the implementation of our method onboard a high-payload-capable quadrotor, experiments that demonstrate some improved performance with our proposed method, relative to the geometric tracking method. Future work could include tests that enable an improvement in robustness and convergence of the MPC-based trajectory planner by using a special structure. Other potential future directions are to estimate the MAV pose via reliable vision-based algorithms so that the aerial vehicle can exploit outdoor and in environments with obstacles.

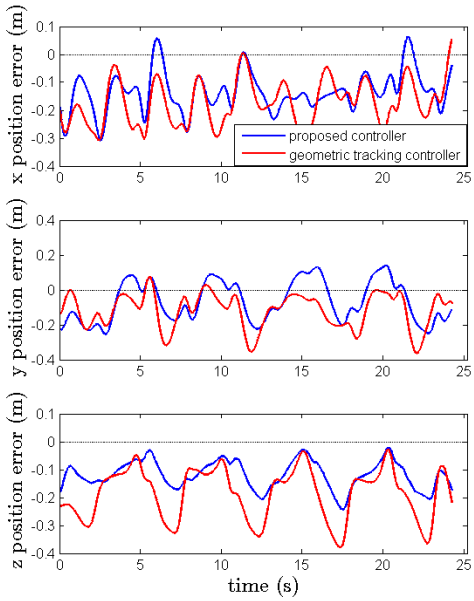


Fig. 5. Resulting response for the eight-shape trajectory. The solid blue line represents the error between quadrotor position and the reference with our proposed control method. The red line is the error with the geometric tracking controller.

## References


[1] F. Fraundorfer, L. Heng *et al.*, "Vision-based autonomous mapping and exploration using a quadrotor MAV," in *Proc.* 2012 *IEEE/RSJ IROS*, 2012, pp. 4557–4564.

[2] L. Heng, L. Meier *et al.*, "Autonomous obstacle avoidance and maneuvering on a vision-guided MAV using on-board processing," in *Proc.* 2011 *IEEE ICRA*, pp. 2472–2477.

[3] R. Ritz, M. W. Müller *et al.*, "Cooperative quadrocopter ball throwing and catching," in *Proc.* 2012 *IEEE/RSJ IROS*, pp. 4972–4978.

[4] F. Augugliaro, S. Lupashin *et al.*, "The flight assembled architecture installation: Cooperative construction with flying machines," *IEEE Control Systems Magazine*, vol. 34, no. 4, pp. 46–64, 2014.

[5] T. Lee, M. Leok *et al.*, "Geometric tracking control of a quadrotor UAV on SE(3)," in *Proc.* 2010 *IEEE CDC*, pp. 5420–5425.

[6] K. Alexis *et al.*, "Switching model predictive attitude control for a quadrotor helicopter subject to atmospheric disturbances," *Control Engineering Practice*, vol. 19, no. 10, pp. 1195–1207.

[7] D. Mellinger and V. Kumar, "Minimum snap trajectory generation and control for quadrotors," in *Proc.* 2011 *IEEE ICRA*, pp. 2520–2525.

[8] A. Franchi, C. Masone *et al.*, "Modeling and control of UAV bearing formations with bilateral high-level steering," *The international Journal of Robotics Research*, vol. 31, no. 12, pp. 1504–1525, 2012.

[9] G. M. Hoffmann, H. Huang *et al.*, "Quadrotor helicopter flight dynamics and control: Theory and experiment," in *Proc.* 2007 *AIAA Guidance, Navigation and Control Conference*, pp. 1–20.

[10] S. Bouabdallah and R. Siegwart, "Full control of a quadrotor," in *Proc.* 2007 *IEEE/RSJ IROS*, pp. 153–158.

[11] ——, "Backstepping and sliding-mode techniques applied to an indoor micro quadrotor," in *Proc.* 2005 *IEEE ICRA*, pp. 47–52.

[12] A. Aswani, P. Bouffard, and C. Tomlin, "Extensions of learning-based model predictive control for real-time application to a quadrotor helicopter," in *Proc.* 2012 *ACC*, pp. 4661–4666.

[13] E. N. Hartley, J. L. Jerez *et al.*, "Predictive control using an FPGA with application to aircraft control," *IEEE Trans. Control Systems Technology*, vol. 22, no. 3, pp. 1006–1017, 2014.

[14] G. S. Schmidt, C. Ebenbauer, and F. Allgöwer, "Output regulation for control systems on SE(n): A separation principle based approach," *IEEE Trans. Automatic Control*, vol. 59, no. 11, pp. 3057–3062, 2014.

[15] ——, "On the differential equation $\dot{\theta} = (\theta^\top - \theta)\theta$ with $\theta \in \mathrm{SO}(n)$," arXiv technical report arXiv:1308.6669, 2013.

[16] J. Mattingley, Y. Wang *et al.*, "Automatic generation of high-speed solvers," *IEEE Control Systems Magazine*, vol. 31, no. 3, pp. 52–65.

[17] M. W. Mueller and R. D'Andrea, "A model predictive controller for quadrocopter state interception," in *Proc.* 2013 *European Control Conference*, Zurich, Switzerland, 2013, pp. 1383–1389.

[18] V. Grabe *et al.*, "The TeleKyb framework for a modular and extendible ROS-based quadrotor control," in *Proc.* 2013 *ECMR*, pp. 19–25.

[19] D. Cabecinhas, R. Cunha *et al.*, "A nonlinear quadrotor trajectory tracking controller with disturbance rejection," *Control Engineering Practice*, vol. 26, pp. 1–10.